Functional analysis of Cdc20 reveals a critical role of CRY box in mitotic checkpoint signaling

Yuqing Zhang[1], Rose Young[2], Dimitriya H Garvanska[3], Chunlin Song[1], Yujing Zhai[4], Ying Wang[4], Hongfei Jiang[1], Jing Fang[1], Jakob Nilsson[3], Claudio Alfieri[2]*, Gang Zhang[1]*

1. Cancer Institute, The Affiliated Hospital of Qingdao University, Qingdao University, Qingdao, China

2. Chester Beatty Laboratories, Structural Biology Division, Institute of Cancer Research, London, UK

3. The NNF Center for Protein Research, University of Copenhagen, Copenhagen, Denmark

4. School of Public Health, Qingdao University, Qingdao, China

* Correspondence to: Gang Zhang, zhanggang_sma@qdu.edu.cn or Claudio Alfieri, claudio.alfieri@icr.ac.uk

Abstract

Accurate chromosome segregation is coordinated by the spindle assembly checkpoint (SAC) through its effector the mitotic checkpoint complex (MCC), to inhibit the anaphase-promoting complex or cyclosome (APC/C). Cdc20 is an essential mitotic regulator since it promotes mitotic exit through activating the APC/C and monitors kinetochore-microtubule attachment through activating the SAC. The proper functioning of Cdc20 requires multiple interactions with APC/C and MCC subunits. To functionally assess each of these interactions within cells requires efficient depletion of endogenous Cdc20, which is highly difficult to achieve by RNAi. Here we generated Cdc20 RNAi sensitive cell lines by CRISPR/Cas9 which display a penetrant metaphase arrest phenotype by a single RNAi treatment. In this null background, we accurately measured the contribution of each known motif of Cdc20 on APC/C and SAC activation. The CRY box, a previously identified degron was found to be critical for the SAC by promoting the MCC formation and stabilizing the interaction between the MCC and APC/C. These data reveal additional regulatory components within the SAC and establish a novel method to interrogate Cdc20 function.

Introduction

Cdc20 is a key subunit of the MCC[1,2], which is produced at unattached kinetochores by the SAC signaling pathway. The MCC binds and inhibits the E3 ligase, APC/C to delay the transition from metaphase to anaphase, thus providing sufficient time for the establishment of stable attachment between kinetochores and microtubules[3]. Cdc20 is the mitotic co-activator of the APC/C and the binding of Cdc20 causes APC/C conformational changes that favor the loading of the E2 ligases UBE2C and UBE2S which brings activated ubiquitin ready for transfer to an APC/C-bound substrate[4]. Besides activating APC/C, Cdc20 recognizes APC/C-targeting sequences or degrons on substrates and facilitates substrates ubiquitination by APC/C[5]. Two Cdc20 molecules are part of the APC/C^{MCC} complex, one in the MCC and the other in the APC/C[6,7,8]. Binding of the MCC to the APC/C interferes with Ube2C binding[7]. Moreover, the MCC component BubR1 interacts with Cdc20$^{APC/C}$ and blocks substrate recognition. Thus, MCC directly inhibits APC/C from ubiquitinating Cyclin B1 and securin hereby causing a mitotic arrest[9,10].

Cdc20 has an unstructured N-terminal region (residues 1-173) and a seven-bladed β-propeller or WD40 domain at the C-terminus (residues 174-470). The N-terminal region harbors motifs binding with Mad1 (BM1), Mad2 (KILR), Apc8 (C box; KILR) and two degrons recognized by APC/C^{Cdh1} (KEN, CRY box)[11,12,13,14,15,16,17]. There are also numerous residues phosphorylated by the mitotic kinases Cdk1, Plk1 and Bub1[18,19,20,21]. The β-propeller domain mainly contains binding pockets for degrons (i.e. D box and KEN box) and other APC/C-recognition sequences (e.g. ABBA motif)[22,23,24]. At the C-terminal end, an IR motif mediates the interaction with Apc3 (for Cdc20$^{APC/C}$) or Apc8A (for Cdc20^{MCC})[7,12,14].

Similar to other mitotic checkpoint proteins like Bub1 or Mad1, Cdc20 is extremely difficult to be efficiently depleted by RNAi to block mitotic progression. It is estimated that the endogenous Cdc20 protein level has to be reduced to less than 5% for the cells to show mitotic arrest[25,26]. On the other hand, complete inactivation of Cdc20 using gene trap method resulted in metaphase arrest and apoptosis afterwards[27]. Thus, how to precisely measure the contribution of each Cdc20 functional motif to APC/C and SAC activation in a clean null background remains a technical challenge.

Previously we generated *Bub1* knockout cell lines by CRISPR/Cas9. These cells are viable due to residual Bub1 protein and are highly sensitive towards Bub1 depletion by RNAi[28]. Using this cell line, we completely removed the residual Bub1 and revealed the distinct roles of Bub1-Mad1 and RZZ-Mad1 on SAC activation as well as the biological significance of separating the kinase activity and phosphatase activity within Bub1 complex[28,29]. Here, we applied a similar strategy for the study of Cdc20. We precisely measured the contribution of each motif on the activation of SAC and APC/C. Though most of our results are in line with the previous studies, we found the disruption of any one of the three APC/C binding motifs on Cdc20 abolished the activation of APC/C in cells which have not been demonstrated before. Furthermore, we discovered that the cryptic degron CRY box was critical for SAC activation, but not for APC/C activation. By structural and functional analysis, we show that the CRY box of $Cdc20^{MCC}$ forms multiple interactions at the interface between MCC and the APC/C to facilitates MCC formation and MCC-mediated APC/C inhibition. Due to the high similarity between the C box and the CRY box, the core sequences of the two motifs are exchangeable to support the function of each motif. The arginine within the CRY box is highly conserved indicating an essential role in SAC across eukaryotic cells.

Results

Generation of *Cdc20* RNAi sensitive cell lines

To achieve a clean background and avoid cell death due to the complete loss of Cdc20, we took a similar strategy as utilized previously for Bub1[28,29] (Supplementary Fig. 1A). We designed three sgRNAs targeting distinct positions on exon 1 and 2 and generated many cell lines with either low or undetectable Cdc20 by CRISPR/Cas9 (Supplementary Fig. 1B-E, Fig. 1A). Since complete inactivation of *Cdc20* causes metaphase arrest and apoptosis[27], we reasoned the survival of the knockout cells without detectable Cdc20 is very likely supported by residual Cdc20 protein beyond detection by western blot. Indeed, Cdc20 peptides were detected by mass spectrometry from the immunoprecipitate with an antibody against the C-terminus of Cdc20 of one such clone, KO3-9 (Supplementary Fig. 1F). All these clones spent extra 30-70 minutes in mitosis than parental cells (Fig. 1B). More importantly, 24 hours after treatment with an siRNA oligo against Cdc20, the majority of mitotic cells from such clones were arrested at metaphase till cell death while parental cells were shortly delayed before entering anaphase. The metaphase arrest in knockout cells was fully rescued by reintroducing RNAi resistant YFP-Cdc20 (Fig. 1C; Fig. 2C-F).

In conclusion, the above results show the successful generation of Cdc20 RNAi sensitive cell lines. Since the clones from sgRNA #3 gave more homogenous results, we decided to characterize these cell lines further.

Cdc20 knockout cell lines are unable to activate the SAC

We first examined the mitotic progression by live cell imaging using a fluorescent histone marker. The results showed that the prolonged mitosis in the knockout cells was due to a metaphase-anaphase transition delay (Supplementary Fig. 2A,B). The

degradation of YFP-Cyclin B1 was much slower in the knockout cells than in parental HeLa cells indicating the delay was caused by the inefficient Cyclin B1 degradation (Supplementary Fig. 2C,D). The slow Cyclin B1 degradation could be a result of less active APC/C^{Cdc20} or increased SAC strength. To discriminate between this we examined SAC strength in the knockout cells. Low dose of nocodazole partially depolymerized microtubules and activated the mitotic checkpoint which arrested the parental HeLa cells in mitosis with a medium time around 585 min. Interestingly, none of the three knockout cell lines were arrested in mitosis after nocodazole treatment (Fig. 1D). Similar results were obtained with paclitaxol, another microtubule toxin which dampened microtubule dynamics and activated mitotic checkpoint (Fig. 1E). When the knockout cells were treated with reversin, an inhibitor of the checkpoint kinase Mps1[30], the mitotic length was not affected while in the parental cells an accelerated mitosis was observed (Fig. 1F). The SAC was fully restored when the knockout cells were supplemented with YFP-Cdc20 indicating the checkpoint defect was caused by the low levels of Cdc20 (Fig. 1G).

In summary, the characterization of the *Cdc20* knockout cell lines indicates that the residual Cdc20 can partially activate APC/C, but not the SAC.

Functional analysis of Cdc20 motifs in the Cdc20 null background

After characterizing the *Cdc20* RNAi sensitive cell lines, we decided to quantify the contribution of each documented Cdc20 interaction to SAC and APC/C activation. A series of Cdc20 mutants were generated according to previous studies (Fig. 2A,B). Localization analysis by immunofluorescence showed all the mutants except Cdc20ΔABBA R, the one lacking the ABBA-binding motif decorated kinetochores (Supplementary Fig. 3A). The knockout cell line 3-9 was used for the functional

analysis of these mutants. KO3-9 cells were synchronized by double thymidine and the RNAi-resistant plasmids expressing YFP-Cdc20 variants were transfected after the first thymidine arrest. RNAi against *Cdc20* was conducted the next day during the second thymidine arrest and live cell imaging was performed 24 hrs later. Unperturbed mitosis and nocodazole challenged mitosis were recorded side by side for each mutant to examine the activity of APC/C and SAC separately.

For unperturbed mitosis, removal of the C-terminal IR motif or the C box individually or combinatorially, which compromises Cdc20 binding to the APC/C, caused metaphase arrest followed by cell death. Similar results were obtained when the cells were treated with nocodazole (Fig. 2C). To confirm that the arrest was caused by failed activation of APC/C but not by a highly active SAC, we lowered the concentration of nocodazole and recorded the time the cells spent in mitosis again. The cells complemented with wild type Cdc20 exited mitosis significantly faster with nocodazole at 15 ng/ml than at 30 ng/ml (medium time 430 min vs 570 min). In contrast cells expressing Cdc20 lacking APC/C interaction motifs arrested for the same amount of time irrespective of nocodazole concentration changes (Supplementary Fig. 3B). Thus the arrest observed with these mutants is due to their lack of APC/C activation.

The Cdc20 mutants defective at BubR1 binding showed accelerated mitosis in both unperturbed mitosis and SAC-activated mitosis. Cdc20ΔKEN box R gave the strongest SAC defect followed by Cdc20ΔD box R and Cdc20ΔABBA R (Fig. 2D). Similarly, both Mad1 and Mad2 binding-defective Cdc20 mutants had fast mitosis in the absence or presence of nocodazole. Cdc20ΔMad2 showed SAC defect as strong as Cdc20ΔKEN box R while Cdc20ΔMad1 displayed a mild SAC defect. Another mutant Cdc20ΔKILR defective at binding with both APC8 and Mad2 exhibited similar mitotic arrest and cell death in unperturbed mitosis and nocodazole-treated mitosis as

Cdc20ΔIR or Cdc20ΔC box indicating its critical role in APC/C activation. We noticed a small pool of cells expressing Cdc20ΔKILR exit mitosis quickly when challenged with nocodazole (Fig. 2E). We also examined the effect of Cdc20 phosphorylation by Cdk1 which has been reported to lower APC/C activity. In line with the previous studies, Cdc20 6A mutant induced accelerated mitosis in the absence and presence of nocodazole. Cdc20ΔKEN mutant did not induce a significantly accelerated or delayed mitosis in either unperturbed mitosis or SAC-activated mitosis arguing that it is not critical for mitosis (Fig. 2F).

The most unexpected phenotype comes from the CRY box, an unconventional degron that is poorly characterized in human somatic cells. In our system Cdc20ΔCRY accelerated an unperturbed mitosis which was due to an abolished SAC as Cdc20ΔCRY complemented cells were not arrested in the presence of nocodazole (Fig. 2F).

Given this surprising result we decided to investigate the CRY box in more detail.

CRY box is required for SAC via multiple interaction with MCC and APC/C

In order to understand the molecular mechanism of how the CRY box participates in SAC-dependent inhibition of the APC/C, we performed a structure-function analysis of this motif based on the APC/C^{MCC} structure determined by cryo-electron microscopy (cryo-EM)[7,31] (Fig. 3A,B). From this structure, the Cdc20^{MCC} CRY box (residues 162-170) forms a loop that precedes the first WD40 repeat (Fig. 3C,D). Two basic residues preceding the core CRY sequence, Cdc20^{MCC} R162 and K163, are in proximity of two acidic residues, E180 and D203 on Cdc20$^{APC/C}$ suggesting that these residues are involved in electrostatic interactions. The CRY box has a U shape with R166 performing the U-turn of the polypeptide chain (Fig. 3C). This specific arrangement is independent from the binding of MCC to the APC/C complex as it is also present in the crystal structure of Cdc20 on its own[22]. The CRY box U-turn conformation is stabilized

by interactions of the conserved R166 and I168 with the first WD40 repeat of $Cdc20^{MCC}$. The CRY motif is wedged in-between the acidic $Cdc20^{APC/C}$ D box receptor region and two BubR1 interacting loops which are juxtaposed. Because of the knot-like shape of this domain we call it $BubR1^{KNOT}$ (Fig. 3C). The $BubR1^{KNOT}$ is formed by the BubR1 first D-box pseudo-degron sequence (residues 224-232) which entangles with the following hydrophobic loop (residues 242-252) (Fig. 3C,D). The CRY motif residues following R162 and K163 are mainly non-polar, and they establish van der Waals interactions with a non-polar region of $Cdc20^{APC/C}$ underneath the D box receptor and the hydrophobic core of the $BubR1^{KNOT}$ structure.

To investigate the function of these interactions, a series of point mutations were designed and their effect on checkpoint was examined. The mutation includes 1), Cdc20 R162E/K163E and Cdc20 E180R/D203R; 2), Cdc20 CRY/3A and individual A mutants; 3), Cdc20 IPS/3A and individual A mutants; 4), Cdc20 CRY individual D mutants; 5) Cdc20 IPS individual D mutants; 6), BubR1 G246D/G247D/A248D (3D) and I242D/I243D/V245D/L249D (4D). Disrupting the electrostatic interaction between $Cdc20^{MCC}$ and $Cdc20^{APC/C}$ by either R162E/K163E or E180R/D203R mutations in Cdc20 significantly impaired the checkpoint (Fig. 4A). Mutations that are designed to unfold either the $Cdc20^{CRY}$ structure (CRY/3A or IPS/3A) or the $BubR1^{KNOT}$ structure (BubR1 3D or 4D) displayed strong SAC defects (Fig. 4B-D). Among the single alanine mutations, R166A alone severely impaired the checkpoint while others showed little or very mild effects (Fig. 4B). For the single aspartic acid mutations in Cdc20, R166D, Y167D and I168D all gave strong SAC defects further supporting a hydrophobic interaction between the CRY box and the surrounding residues (Fig. 4C). The residue Ser170 within the CRY box has been reported to be phosphorylated by Plk1 to facilitate the Cdc20 degradation in G1[20]. The individual alanine or aspartic acid mutation

analysis of the Ser170 on SAC suggested a marginal role of this residue and its phosphorylation in the SAC. Another known post-translational modification which might be invovled in regulating SAC via the interaction with the CRY box is the acetylation of BubR1 K250[32]. However, using the established BubR1 RNAi and rescue method[23], we could not see a meaningful contribution of K250 acetylation in SAC activation as described before[32] (Supplementary Fig. 3C).

The above structure-function analysis indicates that multiple contacts of $Cdc20^{MCC}$ CRY box with $Cdc20^{APC/C}$ and $BubR1^{KNOT}$ stabilize the interaction between MCC and APC/C. To confirm this, we performed immunoprecipitation in HeLa cells expressing YFP tagged wild type Cdc20, Cdc20 R166A, Cdc20 CRY/3A, wild type BubR1, BubR1 3D, BubR1 4D mutants by GFP-trap beads. Western blot analysis showed Cdc20 R166A and CRY/3A mutant were defective at both MCC formation and binding with APC/C. BubR1 3D or 4D mutants were still able to form MCC, though less efficiently than wild type BubR1, and largely lost the interaction with APC/C (Fig. 4E,F). Our data also reveal that R166 is important for MCC formation as predicted by structure analysis that R166 may interact with and stabilize the WD40 domain. The loss of APC/C binding from R166A could be due to a combined effect of impaired MCC formation and misorientation of the CRY box. Conversely, BubR1 3D or 4D mainly affects MCC binding to APC/C^{Cdc20} (Fig. 4E,F). To further confirm the above observation, we reconstituted the APC/C^{Cdc20} complex and the MCC complex (Supplementary Fig. 4). We chose to test the inhibitory effect of MCC formed with either Cdc20 R162E/K163E or BubR1 4D on APC/C^{Cdc20} with Cyclin B1 as the substrate. The assay showed that the MCC formed by wild type components efficiently inhibited APC/C^{Cdc20} while the MCC reconstituted with Cdc20 2E mutant or BubR1 4D mutant did not (Fig. 4G,H). BubR1 4D is much less inhibitory than Cdc20 2E which

is consistent with the more prominent structural role of the former domain in stabilizing the CRY box interaction.

C box is exchangeable with CRY box for APC/C and SAC activation

The core sequence of CRY box (CRYIPS) is highly similar to the C box (DRYIPH) as observed previously[15]. The Apc8 binding residues Arg and Ile in the C box are both present in the CRY box and the above functional analysis revealed a certain tolerance of residue variation on SAC of C165 or S170 within the CRY box. We reasoned that the core sequences of the two boxes could be exchanged without impairing the individual function. Cdc20 mutants with either CRY box replaced by C box or C box replaced by CRY box were constructed and examined for their function. Among wild type Cdc20, 2 x CRY box or 2 x C box mutants, there is no significant difference in the mitotic duration of unperturbed mitosis or SAC-activated mitosis indicating CRY box and C box could compensate the function of each other at their individual positions (Fig. 5A,B).

The functionality of Cdc20 CRY box seems conserved across eukaryotic cells

The CRY box is well conserved from humans to zebra fish while the arginine within the box is highly conserved to worm and yeast (Fig. 5C). Similar pattern was observed for BubR1^{KNOT} as well (Fig. 5D). This suggests that the functionality of the CRY box is conserved with certain sequence variation across species (Fig. 5E).

Discussion

In this study we generated RNAi sensitive cell lines expressing minimal amounts of Cdc20 by CRISPR/Cas9. One interesting feature of these cells is the lack of SAC. The reason behind this is not clear. One possibility is the truncated Cdc20 produced in these cells lost the motif required for MCC formation similar as reported by Tsang et al recently[33]. Likely due to the very low level of Cdc20, APC/C can only be partially activated. With the low APC/C activity, the metaphase-anaphase transition is much delayed, and cells are provided enough time for proper attachment between kinetochores and microtubules. In such scenario, the SAC is not essential any more consistent with the previous study that the SAC became dispensable in cells with UBE2C and UBE2S genetically depleted[34].

Based on this system, we quantified the known motifs on Cdc20 for their contribution to SAC or APC/C activation. It has been revealed that the stable interaction between MCC and APC/C is important for the ligase activity inhibition[16,35]. However, MCC-mediated APC/C inhibition prerequires that APC/C could be activated by the mutated Cdc20. Whether the Cdc20 mutants used in these studies can activate APC/C within cells is not fully disclosed as the residual endogenous protein could activate APC/C to promote mitotic exit or Cyclin B1 degradation even in the presence of the Cdc20 mutants. In the clean background achieved in this study, all three Cdc20 mutants lacking C box, IR motif or KILR motif were not able to activate APC/C and promote mitotic exit in unperturbed mitosis. Cells were arrested at metaphase till apoptosis occurred. Thus, all three APC/C binding motifs are required for the APC/C activation by Cdc20. Our data also supports the role of Cdk1 inhibiting Cdc20 by multiple phosphorylation which was recently questioned[36].

Regarding to the MCC-APC/C binding, several interactions between components from the two complexes are involved including the TPR domain of BubR1 with the UbcH10-binding site on $Apc2^{WHB}$, the IR tail of $Cdc20^{MCC}$ with the C box-binding domain on Apc8A, BubR1/Bub3 and phosphorylation sites on APC/C as well as the lariat-like structure between BubR1 degrons and degron receptors on the two Cdc20 molecules. In this study, multiple novel interactions have been characterized among $Cdc20^{MCC}$, $Cdc20^{APC/C}$ and BubR1. These interactions are mediated by the CRY box which is required for both MCC formation and MCC-APC/C interaction. Individual disruption of each contact caused strong SAC defect suggesting critical role of the CRY box in SAC activation and this was also confirmed by biochemical assays. So, we unveil a new layer of regulation on the MCC-mediated APC/C inhibition by the CRY box in this study. How do the CRY box-mediated interactions cooperate with the other known interactions between the MCC and APC/C for the stable binding of the two protein complexes requires further investigation.

In conclusion, by using CRISPR/Cas9 and RNAi, we reanalyzed the known functional motifs on Cdc20, confirmed their essential roles in APC/C activation, and revealed one novel critical function of the CRY box on MCC inhibition of APC/C. The strategy used here could also be applied to other genes as far as RNAi is preferred but not able to produce a null phenotype alone.

Materials and methods

Cell culture, transfection

HeLa cells were cultivated in DMEM medium (Thermo Fisher Scientific) supplemented with 10% of FBS (Biological Industries) and antibiotics. For Cdc20 RNAi and rescue experiments, cells were seeded in 6 well plate at 50% confluence with thymidine (2.5 mM) in the medium. 24 hours later, cells were released from thymidine and transfected with 450 ng of YFP-Cdc20 expression plasmid with Lipofectamine 2000 (Thermo Fisher Scientific). The next morning, 20 nM of RNAi oligos were transfected with Lipofectamine RNAiMAX (Thermo Fisher Scientific) in the presence of thymidine (2.5 mM). Cells were released from the second thymidine arrest in the following morning and processed for further assays. RNAi oligos targeting Cdc20 (5' CGGAAGACCUGCCGUUACAtt 3'), BubR1 (5' GAUGGUGAAUUGUGGAAUAtt 3') or luciferase (5' CGUACGCGGAAUACUUCGAtt 3') were synthesized from GenePharm.

Cloning

PX459 was used for generating the constructs targeting *Cdc20* according to the original protocol (Ran et al., 2013). Three sequences within exon 1 and 2 selected as Cas9 targeting sites include 5' TGCAAGGACCCCTCCCCCTG 3' (#1), 5' CGCAAAGCCAAGGAAGCCGC 3' (#2) and 5' ACCACTCCTAGCAAACCTGG 3' (#3). For YFP-tagged Cdc20 expression, pcDNA5/FRT/TO N-YFP vector was double digested by restrictive enzymes of KpnI and NotI (Thermo Fisher Scientific). Wild type *Cdc20* was amplified by PCR and inserted into the expression vector according to standard procedures. *Cdc20* mutant constructs were generated with mutation PCR. KOD DNA polymerase (Toyobo) was used for the gene amplification and mutagenesis. Details of the cloning will be provided upon request.

CRISPR/Cas9 mediated gene editing

The construct expressing guide RNA and Cas9 protein was transfected into HeLa cells with Lipofectamine 2000. 48 hours later, cells were under selection with puromycin (1 μg/ml) for two days. After puromycin selection, cells were further cultivated for two more weeks till single clones appeared. Single clones were picked and expanded for further analysis.

Genomic DNA sequencing

Genomic DNA of each knockout cell line was extracted with GeneJET Genomic DNA purification kit (Thermo Fisher Scientific). Primers were designed at 200 nt upstream and downstream of the cutting site on CDC20 exons. 200 ng of genomic DNA was used as template for amplification of interested region by 2 x Taq Plus Master Mix (Vazyme). Amplified genomic DNA was further cloned into pTA2 vector according to manufacturer's instructions (TArget Clone, Toyobo). Six clones were picked and sequenced for each cell line.

Live cell imaging

After RNAi transfection as described in the above, cells were re-seeded into chamber slide (Ibidi) from 6-well plate. Fresh DMEM medium containing thymidine was applied to the chambers for further cultivation. The following morning, cells were released from thymidine arrest. 5 hours later, DMEM medium was replaced by Leibovitz's L-15 medium containing 10% of FBS. Slide was mounted onto Nikon A1 HD25 confocal microscopy (Nikon). 1.68% of laser 488 nm was used for simultaneously YFP signal and DIC imaging. Signals were collected every 10 minutes for a total of 20 hours. NIS-Elements AR Analysis was used for results analysis.

Immunofluorescence

HeLa cells were cultivated on coverslips in 6-well plate and treated as described in the above. Cell fixation and staining were conducted as described previously[29]. Briefly, the cells were washed once by PBS and fixed by 4% paraformaldehyde in PHEM buffer (60 mM PIPES, 25 mM HEPES, pH 6.9, 10 mM EGTA and 4 mM $MgSO_4$) at room temperature for 20 minutes followed by permeabilization with 0.5% Triton X-100/PHEM for 10 minutes. Fixed cells were blocked by 3% BSA/PBST and stained with corresponding antibodies. The antibodies used in this study include GFP (home made in JN lab, 1:500), CENP-C (MBL, PD030, 1:800), Mad1 (Santa Cruz, sc65494, 1:200), Mad2 (home made in JN lab, 1:200), Bub1 (abcam, ab54893, 1:200), Cdc20 (Santa Cruz, sc13162, 1:200), BubR1 (home made in JN lab, 1:200). Fluorophore-labelled secondary antibodies were purchased from Thermo Fisher Scientific (1:1000). ProLong Gold antifade mountant (Thermo Fisher Scientific) was used for the coverslips mounting onto slides. Z-stacks were recorded every 200 nm with a 100 x oil objective and sCMOS camera (DFC9000) equipped on Thunder Imaging System (Leica). Deconvolution and kinetochore protein quantification were performed with LAS X software (Leica).

Immunoprecipitation and Western blot

For Cdc20 and BubR1 immunoprecipitation, 2 μg of plasmid was transfected into HeLa cells in 15 cm dish 48 hours before collection. Cells were synchronized by double thymidine arrest followed by overnight treatment by nocodazole (200 ng/ml). Mitotic cells were shaken off the plate and lysed on ice in lysis buffer containing 10 mM Tris HCl, pH7.4, 150 mM NaCl, 0.5 mM EDTA and 0.5% NP40 with protease and phosphatase inhibitors (Roche). Cell lysate was centrifuged at 17,000 g for 10 min at 4 °C and supernatant was applied to 20 μl of GFP-Trap beads (Chromotek) and shaken for 2 hr at 4 °C. The beads were washed for three times with 0.5 ml lysis buffer each

time and boiled in 50 µl 2 x SDS loading buffer. For Cdc20 knocking out examination, cells from 10 cm dish were collected and lysed in 200 µl of lysis buffer as described in the above. Cell lysate was cleaned by centrifugation and boiled in SDS loading buffer. Quantitative western blot (Odyssey DLx, LI-COR) was performed to examine Cdc20 and interested proteins. Antibodies used include Cdc20 (Santa Cruz, sc-13162; Bethyl, A301-180A), BubR1 (home made in JN lab), Mad1 (Sigma, M8069), Mad2 (home made in JN lab), Apc7 (Santa Cruz, sc-365649), Apc15 (Santa Cruz, sc-398488) and GAPDH (Proteintech, 60004-1). Fluorophore-labeled secondary antibodies include goat anti-mouse IRDye 800CW and goat anti-rabbit IRDye 680CW (LI-COR).

Mass spectrometry analysis

Cells were collected by mitotic shake-off and washed twice with ice-cold PBS. Cell extracts were prepared by resuspending cell pellet in ice-cold lysis buffer (10 mM Tris-HCl, pH 7.5, 150 mM NaCl, 0.5 mM EDTA, pH 8.0, 0.5% NP-40) and incubating on ice for 30 min before centrifugation at 17,000 g for 15 min at 4 °C. The supernatant was transferred to a fresh 1.5 ml microcentrifuge tube. 2 µg Cdc20 antibody (BETHYL,A301-180A) was added into 1.5 mg of cell lysate and the mixture was rotated end-to-end at 4 °C overnight. 40 µl of Protein A/G PLUS-Agarose (Santa Cruz, sc-2003) was applied to the mixture the next morning for 3 hours at 4 °C on the rotating device. The beads were collected by centrifugation at 5000 rpm for 2 minutes at 4 °C and washed 4 times with ice-cold wash buffer (10 mM Tris/Cl pH 7.5, 150 mM NaCl, 0.5 mM EDTA). The beads were resuspended with 40 µl of 2 x sample buffer and boiled for 3 minutes. Immunoprecipitates were separated by SDS-PAGE and sent for mass spectrometry analysis (Hangzhou Cosmos Wisdom Biotechnology).

Protein expression and purification

His-Ubiquitin, His-UBA1 and UbcH10-His

Codon optimised cDNA of human His-ubiquitin, His-UBA1 and UbcH10-His were ordered from GenScript and Addgene and transformed into BL21(DE3)RIL cells. Large scale bacterial culture was shaken at 37 °C, 220 rpm until the OD_{600} reached 0.6 or 0.3 for UBA1. 200 µM of IPTG was added and the culture was continued at 18 ˚C, 180 rpm overnight. The culture was centrifuged at 10,000 x g, 4 °C for 10 mins. The cell pellet was resuspended in 50 mM HEPES pH 7.5, 500 mM NaCl, 5 % glycerol, 0.5 mM TCEP 25 mM imidazole, 5 Units/mL Benzonase, supplemented with an EDTA-free protease inhibitor cocktail (Roche). The cell suspension was sonicated and centrifuged at 40,000 x g for 20 mins. The supernatant was loaded onto a 5 mL HisTrap-HP column (Cytiva) with a 1 mL/min flow rate. Afterwards, the column was washed extensively with wash buffer (50 mM HEPES pH 7.5, 500 mM NaCl, 5 % glycerol, 0.5 mM TCEP and 25 mM imidazole) and the protein was eluted with wash buffer containing 300 mM imidazole. The elute containing His tagged protein was pooled and concentrated before loaded onto a HiLoad 16/600 Superdex 75 pg column (Cytiva) and run with gel filtration buffer (20 mM HEPES pH 7.5, 150 mM NaCl, 0.5 mM TCEP). His-UBA1 was purified as described[37].

MBP-Cdc20, BubR1-GST, Mad2-StrepII, cyclin B1-StrepII, APC/C

Codon optimised cDNA of His-MBP-Cdc20, BubR1-GST and Mad2-StrepII were ordered from GenScript and cyclin B1-StrepII was ordered from GeneArt (Thermo Fisher Scientific), which were all in pFastBac1 vectors and transformed into MultiBac cells for insect cell expression. Baculoviruses for each of these were produced in Sf9 cells and used to infect High Five cells at a cell density of 1.5 x 10^6 cells/mL. For expression of the MCC, the Cdc20, BubR1 and Mad2 baculoviruses coinfected the High Five cells (the Bub3 protein was not included because it is not required for MCC-

mediated APC/C inhibition in vitro[7]). High Five cells were cultured at 27 °C, 130 rpm for 72 hours.

Cdc20 was purified as described[37]. The wt and mutant MCC were all purified in the same way. The cell pellet was resuspended in 50 mM HEPES pH 7.5, 200 mM NaCl, 5 % glycerol, 0.5 mM TCEP, 5 Units/mL Benzonase, supplemented with an EDTA-free protease inhibitor cocktail (Roche). The cell pellets were then sonicated and centrifuged for 1 hour at 55,000 x g. The supernatant was loaded onto a 5 mL StrepTactin Superflow Plus catridge (Qiagen) at a 1 mL/min flow rate and washed with MCC wash buffer (50 mM HEPES pH 7.5, 200 mM NaCl, 0.5 mM TCEP, 5 % glycerol) and then eluted with wash buffer supplemented with 2.5 mM desthiobiotin. The fractions containing MCC were pooled and loaded onto a 5 mL GSTrap HP column (Cytiva) using a 0.5 mL/min flow rate. After extensive washing with MCC wash buffer the MCC was then eluted with wash buffer supplemented with 10 mM glutathione. The pooled fractions were incubated on ice with TEV and HRV-3C proteases for 4 hours and then injected into a Superose 6 increase 10/300 GL (Cytiva). Fractions containing the MCC were pooled and concentrated.

The cyclin B1 cell pellet was resuspended in 50 mM HEPES pH 8.0, 500 mM NaCl, 5 % glycerol, 0.5 mM TCEP, 5 Units/mL Benzonase supplemented with an EDTA-free protease inhibitor cocktail (Roche). After sonication the lysed cells were centrifuged at 55,000 x g for 1 hour. The supernatant was loaded onto a 5 mL StrepTactin Superflow Plus catridge (Qiagen) using a 1 mL/min flow rate and washed with cyclin B1 wash buffer (50 mM HEPES pH 8.0, 500 mM NaCl, 5 % glycerol, 0.5 mM TCEP) and eluted with wash buffer supplemented with 2 mM desthiobiotin. Fractions were concentrated and loaded onto a HiLoad 16/600 Superdex 200 pg column (Cytiva).

Recombinant human APC/C with a phosphomimic mutation in Apc1 was expressed in High Five insect cells. The High Five cells were infected with three separate baculoviruses, one containing Apc5, Apc8, Apc10, Apc13, Apc15, Apc2 and strep tagged Apc4 (gifted by David Barford's lab). The second contained Apc1 phosphomimic mutant (Apc1 Ser364Glu, Ser372Glu, Ser373Glu, Ser377Glu)[38] and Apc11 and the third with Apc3, Apc6, Apc7, Apc12 and Apc16. High Five cells were infected at a cell density of 2 x 10^6 and cultured at 27 °C, 130 rpm for 72 hours.

The APC/C cell pellet was resuspended in 50 mM HEPES pH8.3, 250 mM NaCl, 5 % glycerol, 2 mM DTT, 1 mM EDTA, 0.1 mM PMSF, 2 mM Benzamidine, 5 units/mL Benzonase supplemented with an EDTA-free protease inhibitor (Roche). Cells were sonicated and then centrifuged at 48,000 x g for 1 hour. The supernatant was loaded to a 5 mL StrepTactin Superflow Plus cartridge (Qiagen) using a 1 mL/min flow rate. The column was washed extensively with APC/C wash buffer (50 mM HEPES pH 8.3, 250 mM NaCl, 5 % glycerol, 2 mM DTT, 1 mM EDTA, 2 mM Benzamidine) and eluted with wash buffer supplemented with 2.5 mM desthiobiotin (IBA-Lifesciences). Fractions containing APC/C were incubated overnight with tobacco etch virus (TEV) protease then diluted two-fold with saltless Buffer A (20 mM HEPES pH 8.0, 125 mM NaCl, 5 % glycerol, 2 mM DTT, 1 mm EDTA). This was loaded onto a 6 mL ResourceQ anion-exchange column (GE Healthcare) and the column washed with buffer A. The APC/C was eluted with a gradient of Buffer B (20 mM HEPES pH 8.0, 1 M NaCl, 5 % glycerol, 2 mM DTT, 1 mM EDTA). Concentrated APC/C was centrifuged (Optima TLX Ultracentrifuge) at 40,000 rpm for 30 minutes.

Ubiquitination assay

50 nM APC/C, 50 nM Cdc20, 200 nM cyclin B1, 30 nM UBA1, 20 µM Ubiquitin, 5 mM ATP, 0.25 mg/mL BSA and 250 nM UbcH10 were mixed in a 15 µL reaction

volume with reaction buffer: 40 mM HEPES pH 8.0, 0.6 mM DTT, 10 mM $MgCl_2$. 270 nM of each MCC construct was added into its respective reaction. The reaction mixture was incubated at 25 °C for 15 minutes. Samples were taken at 0 and 15 minutes and the reaction was terminated with SDS/PAGE loading dye. The reaction mixture was run on a 4-12% NuPAGE Bis-Tris gel and transferred to a nitrocellulose membrane for Western blotting. Blocking was carried out in 5% BSA-TBST and washed in 1 x TBST. Ubiquitin modified cyclin B1 was detected using an anti-cyclinB1 mAb (ABclonal, A19037) at a 1:2,000 dilution, and HRP-conjugated goat anti-rabbit secondary antibody (Abcam, ab205718) at a 1:10,000 dilution. The membrane was incubated with ECL, detected using the ImageQuant 800 (Amersham) and quantified using ImageJ.

References

1. Sudakin, V., Chan, G.K. & Yen, T.J. Checkpoint inhibition of the APC/C in HeLa cells is mediated by a complex of BUBR1, BUB3, CDC20, and MAD2. *J. Cell Biol.* **154**, 925-936 (2001).

2. Chao, W.C.H., Kulkarni, K., Zhang, Z., Kong, E.H. & Barford, D. Structure of the mitotic checkpoint complex. *Nature* **484**, 208-213 (2012).

3. Musacchio, A. The molecular biology of spindle assembly checkpoint signaling dynamics. *Curr. Biol.* **25**, R1002-1018 (2015).

4. Chang, L.-F., Zhang, Z., Yang, J., McLaughlin, S.H. & Barford, D. Molecular architecture and mechanism of the anaphase-promoting complex. *Nature* **513**, 388-393 (2014).

5. Davey, N.E. & Morgan, D.O. Building a regulatory network with short linear sequence motifs: lessons from the degrons of the anaphase-promoting complex. *Mol. Cell* **64**, 12-23 (2016).

6. Izawa, D. & Pines, J. The mitotic checkpoint complex binds a second CDC20 to inhibit active APC/C. *Nature* **517**, 631-634 (2015).

7. Alfieri, C. et al. Molecular basis of APC/C regulation by the spindle assembly checkpoint. *Nature* **536**, 431-436 (2016).

8. Yamaguchi, M. et al. Cryo-EM of mitotic checkpoint complex-bound APC/C reveals reciprocal and conformational regulation of ubiquitin ligation. *Mol. Cell* **63**, 593-607 (2016).

9. Kapanidou, M., Curtis, N.L. & Bolanos-Garcia, V.M. Cdc20: at the crossroads between cheomosome segregation and mitotic exit. *Trends Biochem. Sci.* **42**, 193-205 (2017).

10. Alfieri, C., Zhang, S. & Barford, D. Visualizing the complex functions and mechanisms of the anaphase promoting complex/cyclosome (APC/C). *Open Biol*. **7**, 170204 (2017).

11. Pfleger, C.M. & Kirschner, M.W. The KEN box: an APC recognition signal distinct from the D box targeted by Cdh1. *Genes Dev*. **14**, 655-665 (2000).

12. Schwab, M., Neutzner, M., Möcker, D. & Seufert, W. Yeast Hct1 recognizes the mitotic cyclin Clb2 and other substrates of the ubiquitin ligase APC. *EMBO J*. **20**, 5165-5175 (2001).

13. Zhang, Y. & Lees, E. Identification of an overlapping binding domain on Cdc20 for Mad2 and anaphase-promoting complex: model for spindle checkpoint regulation. *Mol. Cell Biol*. **21**, 5190-5199 (2001).

14. Vodermaier, H.C., Gieffers, C., Maurer-Stroh, S., Eisenhaber, F. & Peters, J.-M. TPR subunits of the anaphase-promoting complex mediate binding to the activation protein CDH1. *Curr. Biol*. **13**, 1459-1468 (2003).

15. Reis, A., Levasseur, M., Chang, H., Elliott, D.J. & Jones, K.T. The CRY box: a second APC^{cdh1}-dependent degron in mammalican cdc20. *EMBO Rep*. **7**, 1040-1045 (2006).

16. Izawa, D. & Pines, J. Mad2 and the APC/C compete for the same site on Cdc20 to ensure proper chromosome segregation. *J. Cell Biol*. **199**, 27-37 (2012).

17. Ji, Z., Gao, H., Jia, L., Li, B. & Yu, H. A sequential multi-target Mps1 phosphorylation cascade promotes spindle checkpoint signaling. *Elife* **6**, e22513 (2017).

18. Yudkovsky, Y., Shteinberg, M., Listovsky, T., Brandeis, M. & Hershko, A. Phosphorylation of Cdc20/fizzy negatively regulates the mammalian cyclosome/APC in the mitotic checkpoint. *Biochem. Biophys. Res. Commun*. **271**, 299-304 (2000).

19. D'Angiolella, V., Mari, C., Nocera, D., Rametti, L. & Grieco, D. The spindle checkpoint requires cyclin-dependent kinase activity. *Genes Dev*. **17**, 2520-2525 (2003).

20. Hyun, S.-Y., Sarantuya, B., Lee, H.-J. & Jang, Y.-J. APC/C(Cdh1)-dependent degradation of Cdc20 requires a phosphorylation on CRY-box by Polo-like kinase-1 during somatic cell cycle. *Biochem. Biophys. Res. Commun*. **436**, 12-18 (2013).

21. Jia, L., Li, B. & Yu, H. The Bub1-Plk1 kinase complex promotes spindle checkpoint signalling through Cdc20 phosphorylation. *Nat. Commun.* **7**, 10818 (2016).

22. Tian, W., Li, B., Warrington, R., Tomchick, D.R., Yu, H. & Luo, X. Structural analysis of human Cdc20 supports multisite degron recognition by APC/C. *Proc. Natl. Acad. Sci. U S A*. **109**, 18419-18424 (2012).

23. Di Fiore, B. et al. The ABBA motif binds APC/C activators and is shared by APC/C substrates and regulators. *Dev. Cell* **32**, 358-372 (2015).

24. Diaz-Martinez, L. et al. The Cdc20-binding Phe box of the spindle checkpoint protein BubR1 maintains the mitotic checkpoint complex during mitosis. *J. Biol. Chem*. **290**, 2431-2443 (2015).

25. Wolthuis, R. et al. Cdc20 and Cks direct the spindle checkpoint-independent destruction of cyclin A. *Mol. Cell* **30**, 290-302 (2008).

26. Baumgarten, A.J., Felthaus, J. & Wäsch, R. Strong inducible knockdown of APC/C^{Cdc20} does not cause mitotic arrest in human somatic cells. *Cell Cycle* **8**, 643-646 (2009).

27. Li, M., York, J.P. & Zhang, P. Loss of Cdc20 causes a securin-dependent metaphase arrest in two-cell mouse embryos. *Mol. Cell Biol*. **27**, 3481-3488 (2007).

28. Zhang, G. et al. Efficient mitotic checkpoint signaling depends on integrated activities of Bub1 and the RZZ complex. *EMBO J*. **38**, e100977 (2019).

29. Wang, L. et al. Spatial separation of phosphatase and kinase activity within the Bub complex is required for proper mitosis. *J. Mol. Cell Biol*. **14**, mjac062 (2023).

30. Santaguida, S., Tighe, A., D'Alise, A.M., Taylor, S.S. & Musacchio, A. Dissecting the role of MPS1 in chromosome biorientation and the spindle checkpoint through the small molecule inhibitor reversine. *J. Cell Biol*. **190**, 73-87 (2010).

31. Alfieri, C., Tischer, T. & Barford, D. A unique binding mode of Nek2A to the APC/C allows its ubiquitination during prometaphase. *EMBO Rep*. **21**, e49831 (2020).

32. Choi, E., Choe, H., Min, J., Choi, J.Y., Kim, J. & Lee, H. BubR1 acetylation at prometaphase is required for modulating APC/C activity and timing of mitosis. *EMBO J*. **28**, 2077-2089 (2009).

33. Tsang, M.J. & Cheeseman, I.M. Alternative Cdc20 translational isoforms tune mitotic arrest duration. *Nature* **617**, 154-161 (2023).

34. Wild, T., Larsen, M.S.Y., Narita, T., Schou, J., Nilsson, J. & Choudhary, C. The spindle assembly checkpoint is not essential for viability of human cells with genetically lowered APC/C activity. *Cell Rep*. **14**, 1829-1840 (2016).

35. Hein, J.B. & Nilsson, J. Stable MCC binding to the APC/C is required for a functional spindle assembly checkpoint. *EMBO Rep*. **15**, 264-272 (2014).

36. Bancroft, J. et al. PP1 promotes cyclin B destruction and the metaphase-anaphase transition by dephosphorylating CDC20. *Mol. Biol. Cell* **31**, 2315-2330 (2020).

37. Berndsen, C.E. & Wolberger, C. A spectrophotometric assay for conjugation of ubiquitin and ubiquitin-like proteins. *Anal. Biochem*. **418**, 102-110 (2011).

38. Zhang, S. et al. Molecular mechanism of APC/C activation by mitotic phosphorylation. *Nature* **533**, 260-264 (2016).

Acknowledgements

GZ is supported by the National Natural Science Foundation of China (31970666) and Taishan Scholar Project (tsqn201812054) from Shandong, China. CA and RY are supported by the Sir Henry Dale Fellowship 215458/Z/19/Z. RY is also supported by the Institute of Cancer Research (ICR), grant number allocated is GFR005X. We acknowledge Jing Yang, Ziguo Zhang and David Barford, for helping with the APC/C baculovirus generation.

Author contributions

YZ conducted all the cloning, cell line generation and function analysis. RY purified the recombinant protein complexes and did ubiquitination assay. DHG did Cdc20 and BubR1 immunoprecipitation. CS, YZ, YW, HJ assisted YZ on data collection and analysis. JF provided constructive advices for the project. JN wrote the manuscript together with CA and GZ. CA did structural analysis and supervised the whole project with GZ.

Competing interests

The authors declare no interest conflict in this study.

Figure legends

Figure 1 Generation of RNAi-sensitive *CDC20* knockout cell lines by CRISPR/Cas9

A) Cdc20 in knockout cells from three sgRNAs was examined by western blot with an antibody targeting Cdc20 C-terminal region.

B) The time from NEBD to mitotic exit of the knockout cells. Each circle represents a single cell from NEBD to anaphase. Red line indicates the medium time with the number shown on top. Representative experiment of two independent experiments is shown.

C) The time from NEBD to mitotic exit of the knockout cells after depleting the residual endogenous Cdc20 by RNAi. Each circle represents a single cell from NEBD to cell death or mitotic exit. Red dots are the cells died after the metaphase arrest. Red line indicates the medium time with the number shown on top. Representative experiment of two independent experiments is shown.

D-G) The time from NEBD to exit of HeLa cells and Cdc20 knockout cells after different treatment. D) The cells were treated with nocodazole. E) The cells were treated with pacli-taxol. F) The cells were treated with reversin. G) Knockout cells were supplemented with YFP-Cdc20 and treated with nocodazole.

Figure 2 Functional analysis of Cdc20 in the null background

A) Schematic of the positions of the motifs or phosphorylated sites analysed in this study. B) Mutation details and known functions of the motifs or phosphorylated sites in this study. C-F) The time from NEBD to anaphase (left) or from NEBD to mitotic exit in the presence of nocodazole (right) of the knockout cells complemented with wild type or mutant YFP-Cdc20 after depleting the residual endogenous Cdc20 by RNAi.

Each circle represents a single cell from NEBD to anaphase. Red circle means cell died after mitotic arrest. Red line indicates the medium time with the number shown on top. Representative experiment of two independent experiments is shown. Mann-Whitney u-test was applied. ns means not significant. *** means P<0.001. ns means not significant.

Figure 3 Structure analysis of the CRY motif of Cdc20^{MCC} in the context of MCC-APC/C

A-B) Two views of the APC^{MCC} complex (PDB ID: 6TLJ, Alfieri et al., 2020), the APC/C is shown as surface, the MCC subunits and Cdc20$^{APC/C}$ are shown as cartoon. C) Close-up on the Cdc20^{MCC} CRY box region (from B), interacting with Cdc20$^{APC/C}$ and BubR1^{KNOT} domain. The surface electrostatic potential is shown for the Cdc20$^{APC/C}$. D) Another close-up view showing the composite interface made of Cdc20$^{APC/C}$ and BubR1^{KNOT} domain, which recognises the Cdc20^{MCC} CRY box. Relevant residues are depicted in C and D.

Figure 4 Functional analysis of the interactions with CRY box

A-D) The time from NEBD to mitotic exit in the presence of nocodazole of the knockout cells complemented with wild type or mutant YFP-Cdc20 after depleting the residual endogenous Cdc20 by RNAi or HeLa cells complemented with wild type or mutant YFP-BubR1 after depleting of endogenous BubR1 by RNAi. Each circle represents a single cell from NEBD to mitotic exit. Red line indicates the medium time with the number shown on top. Representative experiment of two independent experiments is shown. Mann-Whitney u-test was applied. ns means not significant. **** means P<0.0001; * means P<0.1; ns means not significant. A) Wild type Cdc20

or R162, K163, E180, D203 mutants were examined for SAC activity. B) Wild type Cdc20 or CRYIPS alanine mutants were examined for SAC activity. C) Wild type Cdc20 or CRYIPS aspartic acid mutants were examined for SAC activity. D) Wild type BubR1 or 3D, 4D mutants were examined for SAC activity. E) Immunoprecipitation was performed using GFP-trap beads in HeLa cells expressing the corresponding YFP-Cdc20 constructs. Quantitative western blot was conducted with corresponding antibodies. Representative experiment of two independent experiments was shown. F) Immunoprecipitation was performed using GFP-trap beads in HeLa cells expressing the corresponding YFP-BubR1 constructs. Quantitative western blot was conducted with corresponding antibodies. Representative experiment of two independent experiments was shown. G) Ubiquitination of Cyclin B1 by APC/C^{Cdc20} after 15 minutes with and without the wild type MCC or with the MCC containing Cdc20 R162E/K163E (2E) or the MCC containing BubR1 I242D/I243D/V245D/L249D (4D). H) Quantification of the Cyclin B1 ubiquitination assay after 15 minutes. The data shown is the mean value ± S.D. of 3 independent experiments. *** means $P<0.0005$, ** means $P<0.005$, the P values were calculated using a two tailed unpaired t-test.

Figure 5 The C box and CRY box are exchangeable for their proper functioning

A) Schematic showing the designing of C box and CRY box exchanging. B) The time from NEBD to anaphase (unperturbed) or from NEBD to mitotic exit in the presence of nocodazole of the knockout cells complemented with wild type or engineered YFP-Cdc20 after depleting the residual endogenous Cdc20 by RNAi. Each circle represents a single cell from NEBD to anaphase or to mitotic exit. Red line indicates the medium time with the number shown on top. Representative experiment of two independent experiments is shown. Mann-Whitney u-test was applied. ns means not significant. C,D)

sequence alignments showing the conservation of Cdc20 CRY BOX (C) and BubR1 KNOT domain (D). E) Cartoon highlighting the critical role of the CRY box in mitotic checkpoint signaling. Top left: kinetochore (yellow circle) not attached by spindle microtubule (green line) organized by centrosome (grey squares) activates the spindle assembly checkpoint; Bottom left: MCC complex is generated from the unattached kinetochore. The CRY box is required for the complex formation. Right: Stable interaction between MCC and APC/C requires the multiple interactions mediated by the CRY box.

Supplementary Figure 1 Characterization of *CDC20* knockout cell lines

A) Cartoon showing the strategy of combining CRISPR/Cas9 and RNAi to achieve a clean background.

B) Schematic showing the target positions of three sgRNAs. Blue rectangles indicate exons and gray ones are introns.

C) Genomic sequencing chromatography of parental cells and the knockout cells from sgRNA #3.

D) Western blot analysis of the checkpoint proteins and APC/C proteins in knockout cells from sgRNA #3. Mitotic cells were collected and analyzed by quantitative western blot with corresponding antibodies.

E) Kinetochore localization of checkpoint proteins in parental cells and knockout cells from sgRNA #3. Mitotic cells were fixed and stained by the corresponding antibodies.

F) Cdc20 peptides identified by mass spectrometry of the immunoprecipitate with Cdc20 antibody against C-terminal region from KO3-9 cells.

Supplementary Figure 2 *Cdc20* knockout cells display a metaphase-anaphase transition delay due to slow degradation of Cyclin B1

A) The mitotic progress was recorded in HeLa cells or *CDC20* knockout cells expressing YFP-H3. The time from NEBD to metaphase (left) and from metaphase to anaphase (right) were analyzed and presented separately. Each circle represents a single cell from NEBD to metaphase or from metaphase to anaphase. Red line indicates the medium time with the number shown on top. Representative experiment of two independent experiments is shown.

B) Representative stills of A).

C) Plot showing YFP-Cyclin B1 degradation from NEBD till anaphase in HeLa cells or *CDC20* knockout cells. The average intensity from 30 cells is presented on each time point. The intensity at time 0 is set to 1. Representative experiment of two independent experiments is shown.

D) Representative stills of C).

Supplementary Figure 3 Characterization of Cdc20 mutants on localization and checkpoint activity

A) Knockout cells were transfected with YFP-Cdc20 constructs and siRNA oligos against Cdc20. Nocodazole treated cells were fixed and stained with corresponding antibodies. B) The time from NEBD to mitotic exit in the presence of nocodazole at two different concentrations of the knockout cells complemented with wild type or mutant YFP-Cdc20 after depleting the residual endogenous Cdc20 by RNAi. Red circle means cell died after mitotic arrest. C) The time from NEBD to mitotic exit in the presence of nocodazole of HeLa cells complemented with wild type or mutant YFP-BubR1 after depleting the endogenous BubR1 by RNAi. Each circle represents a single cell from NEBD to mitotic exit. Red line indicates the medium time with the number

shown on top. Representative experiment of two independent experiments is shown. Mann-Whitney u-test was applied. ** means P<0.01; ns means not significant.

Supplementary Figure 4 Reconstitution of MCC and APC/C

Biochemical reconstitutions of the MCC complexes and the APC/C. A) A chromatogram of MCC^{Wt} from size exclusion chromatography (top). The calibration standards are shown in grey. MCC^{Wt} elutes between 12 and 16 mL. The second peak at 18.5 mL accounts for both 3C-GST and tev used to cleave tags from all three subunits. Coomassie stained gel of the eluted fractions (bottom). B-D) SDS-PAGE of the reconstituted MCC complexes used in this study. E) SDS-PAGE of the reconstituted APC/C.

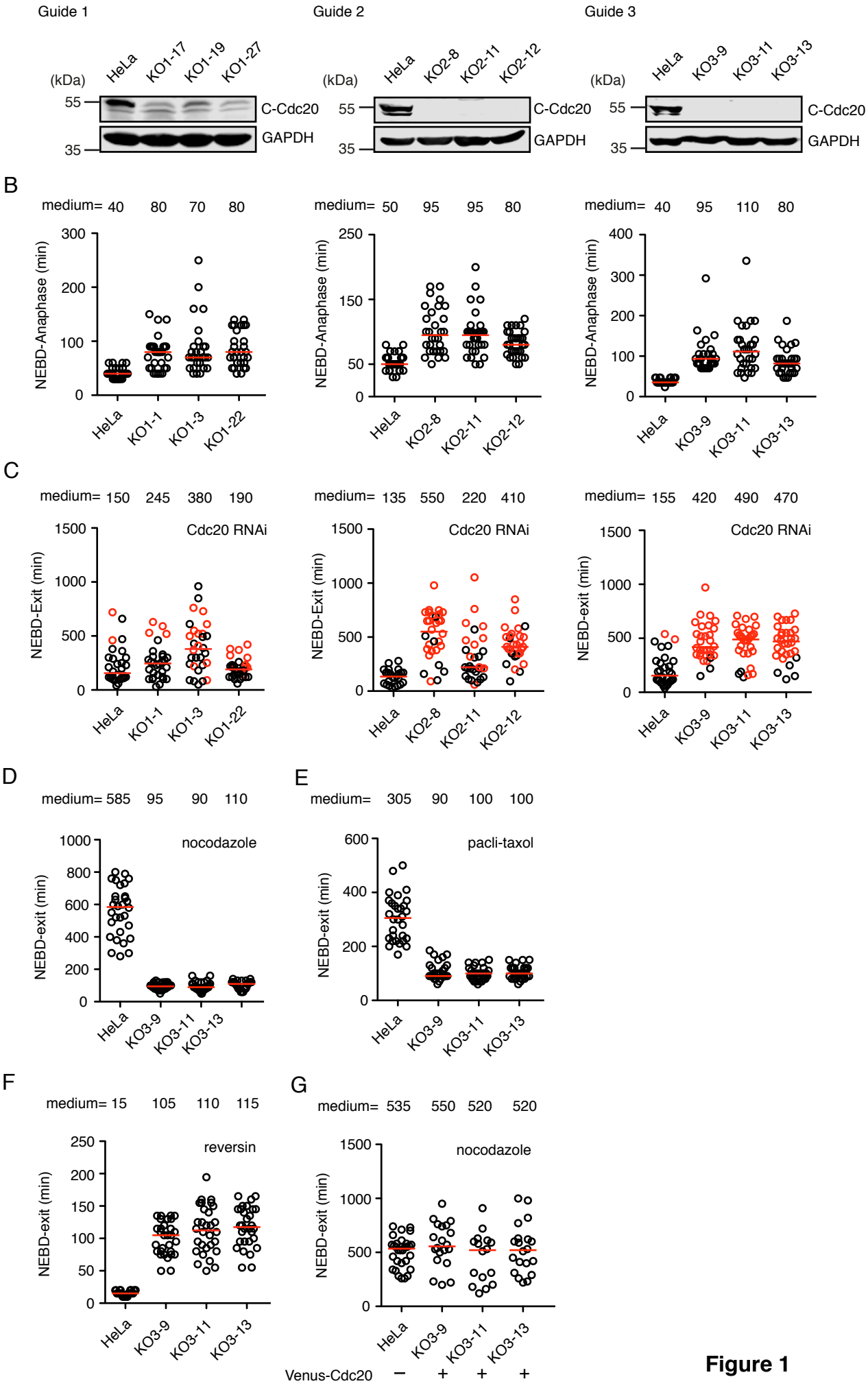

Figure 1

A

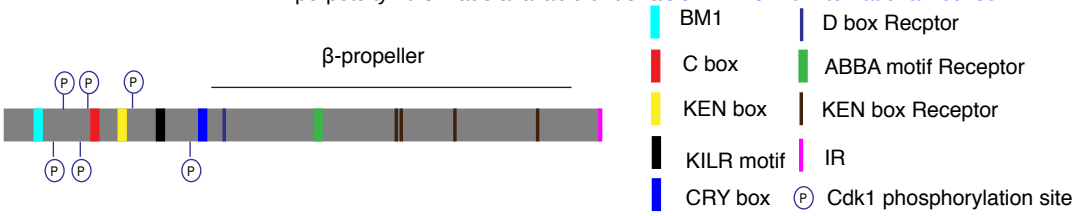

B

Mutant name	Mutation/deletion	Defect
Cdc20ΔIR	Δ498-499	Prevents APC/C binding
Cdc20ΔC box	Δ77-79	Prevents APC/C binding
Cdc20ΔC box ΔIR	Δ77-79; Δ498-499	Prevents APC/C binding
Cdc20ΔD box R	D177A	Prevents BubR1 binding
Cdc20ΔABBA R	R262S	Prevents BubR1 binding
Cdc20ΔKEN box R	N329A/N331A/T377A/R445A	Prevents BubR1 binding
Cdc20ΔMad1	Δ27-31	Prevents Mad1 binding
Cdc20ΔKILR	K129A/I130A/L131A/R132A	Prevents APC/C binding; Prevents Mad2 binding
Cdc20ΔMad2	R132A	Prevents Mad2 binding
Cdc20ΔCRY box	Δ165-167	Prevents degradation
Cdc20 6A	S41A/T55A/T59A/T70A/T106A/T157A	Prevents Cdc20 phosphorylation by Cdk1
Cdc20 ΔKEN	K97A/E98A/N99A	Prevents degradation

C

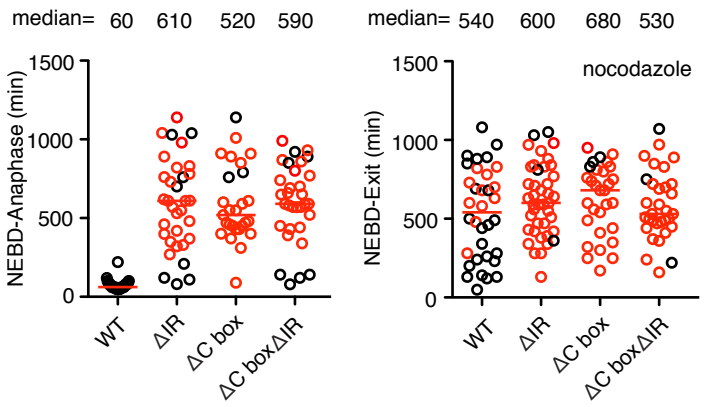

D

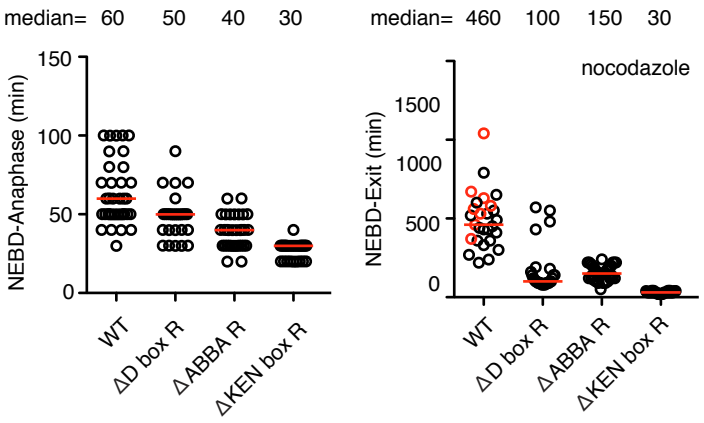

E

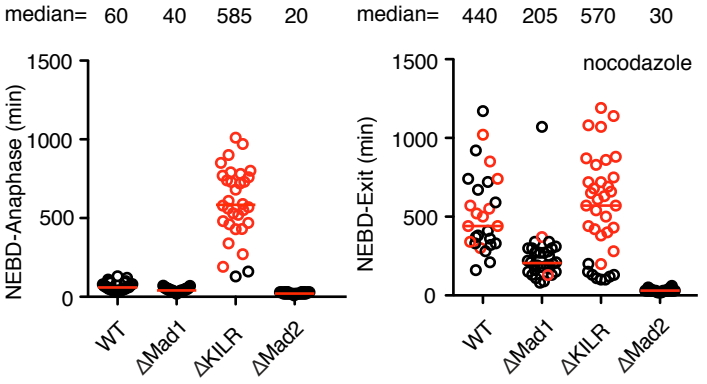

F

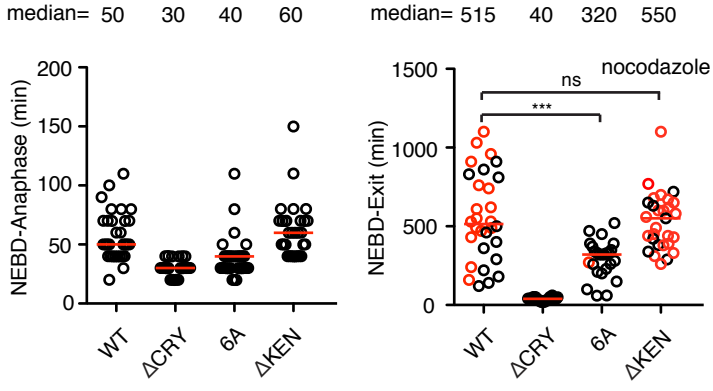

Figure 2

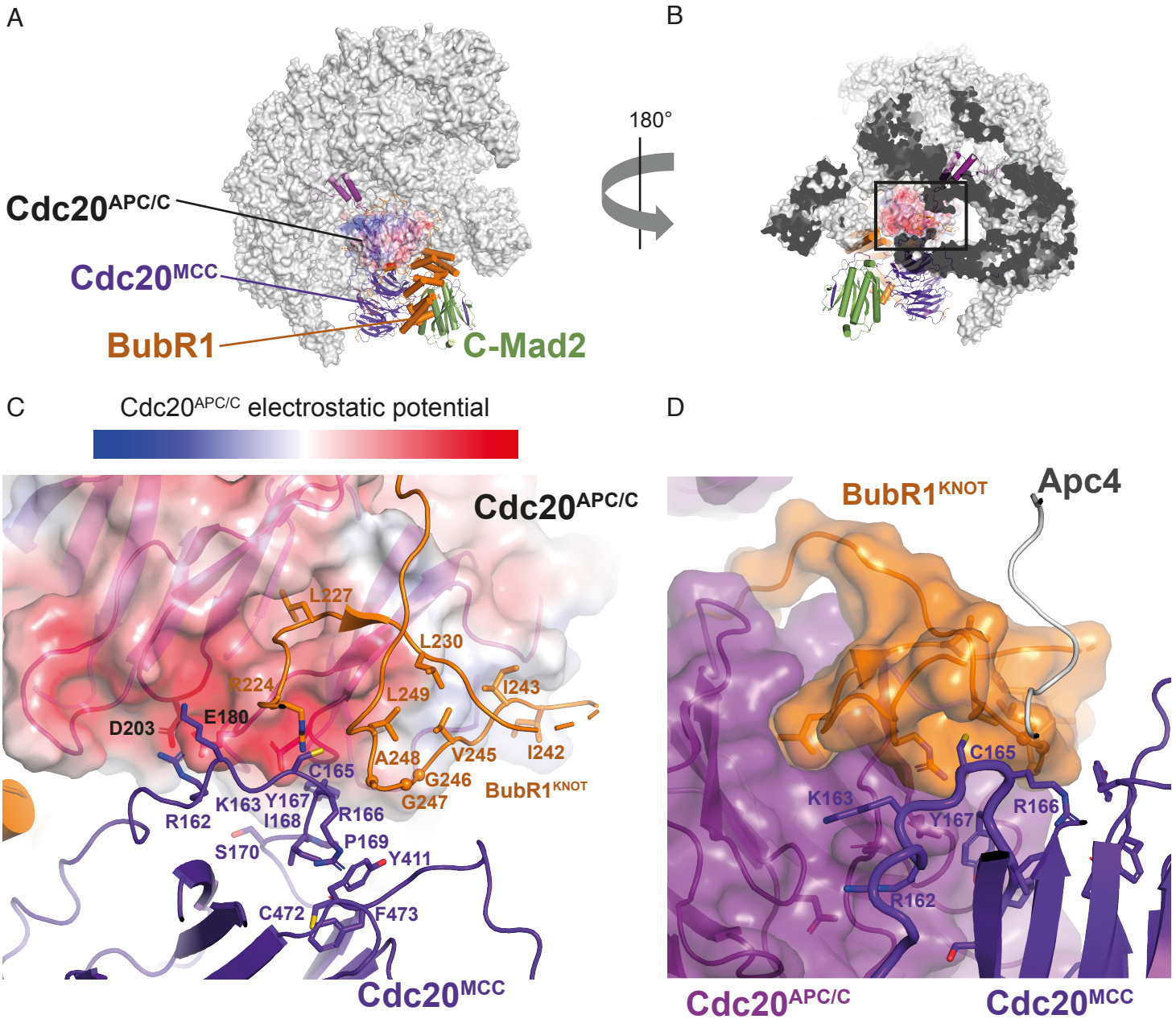
A
Cdc20APC/C
Cdc20MCC
BubR1
C-Mad2
B
180°
C
Cdc20APC/C electrostatic potential
Cdc20APC/C
L227
L230
R224
L249
I243
D203
E180
A248
V245
I242
C165
G246
BubR1KNOT
G247
K163
Y167
R162
I168
R166
P169
S170
Y411
C472
F473
Cdc20MCC
D
BubR1KNOT
Apc4
C165
K163
R166
Y167
R162
Cdc20APC/C
Cdc20MCC

Figure 3

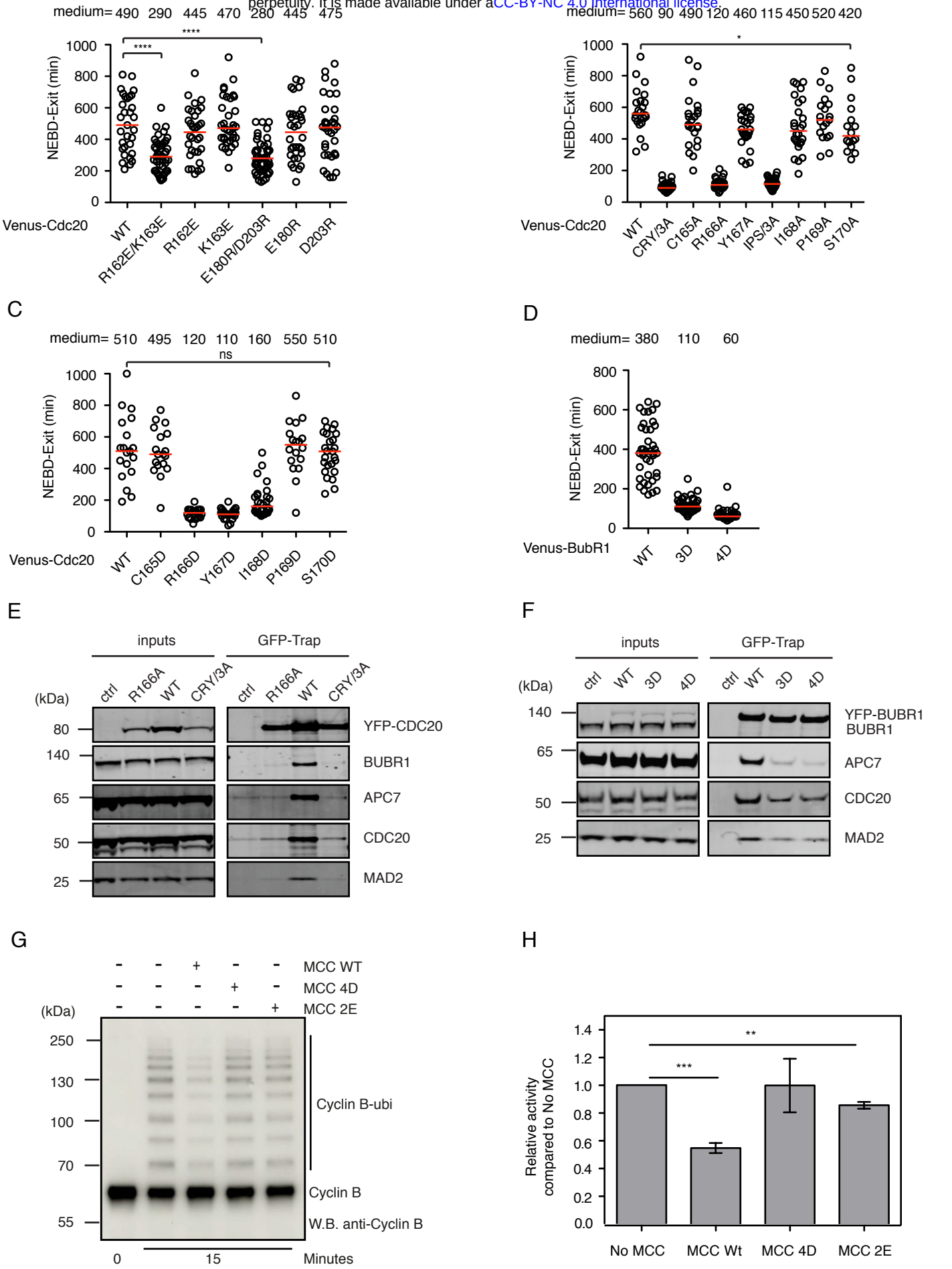

Figure 4

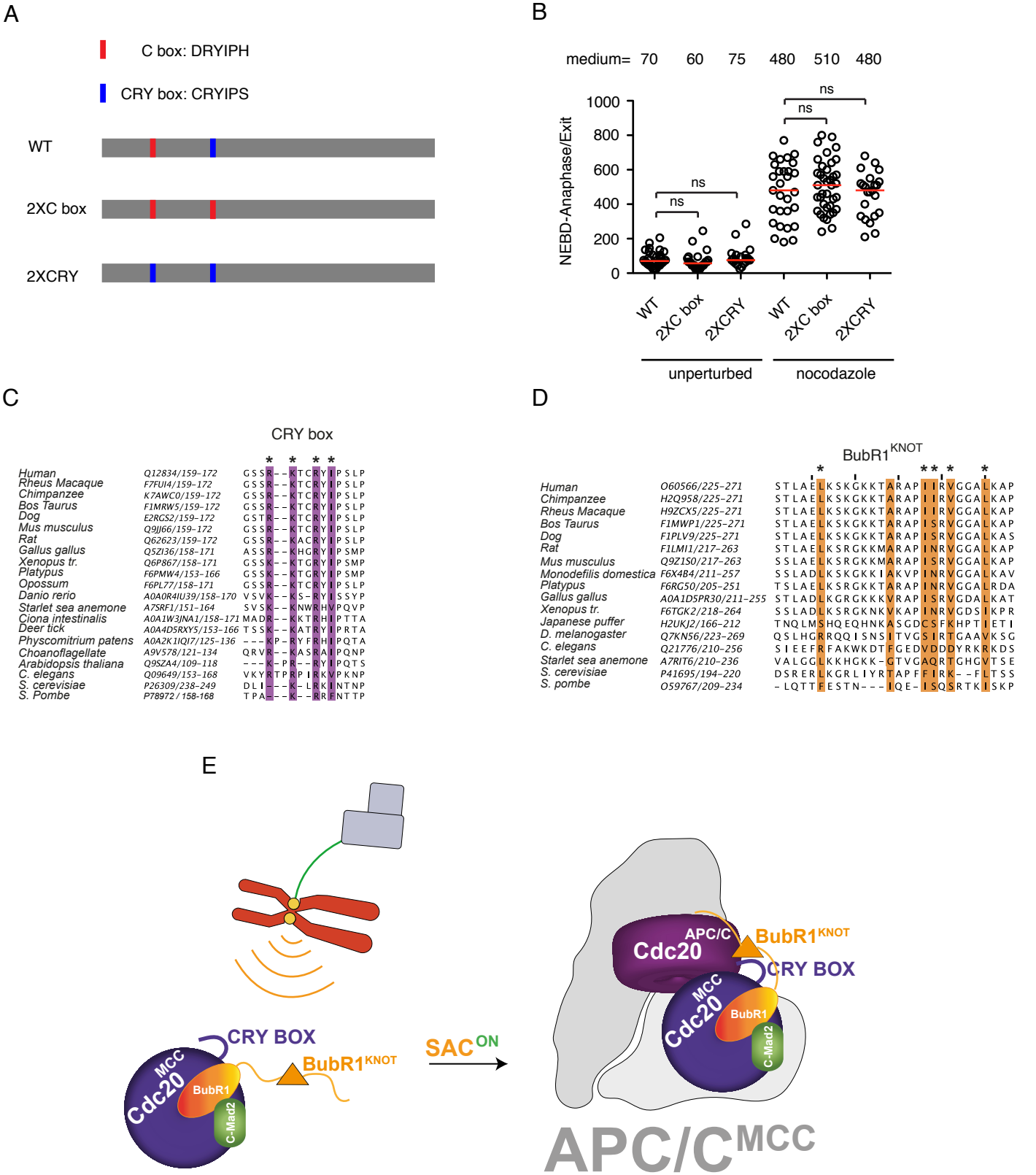

Figure 5

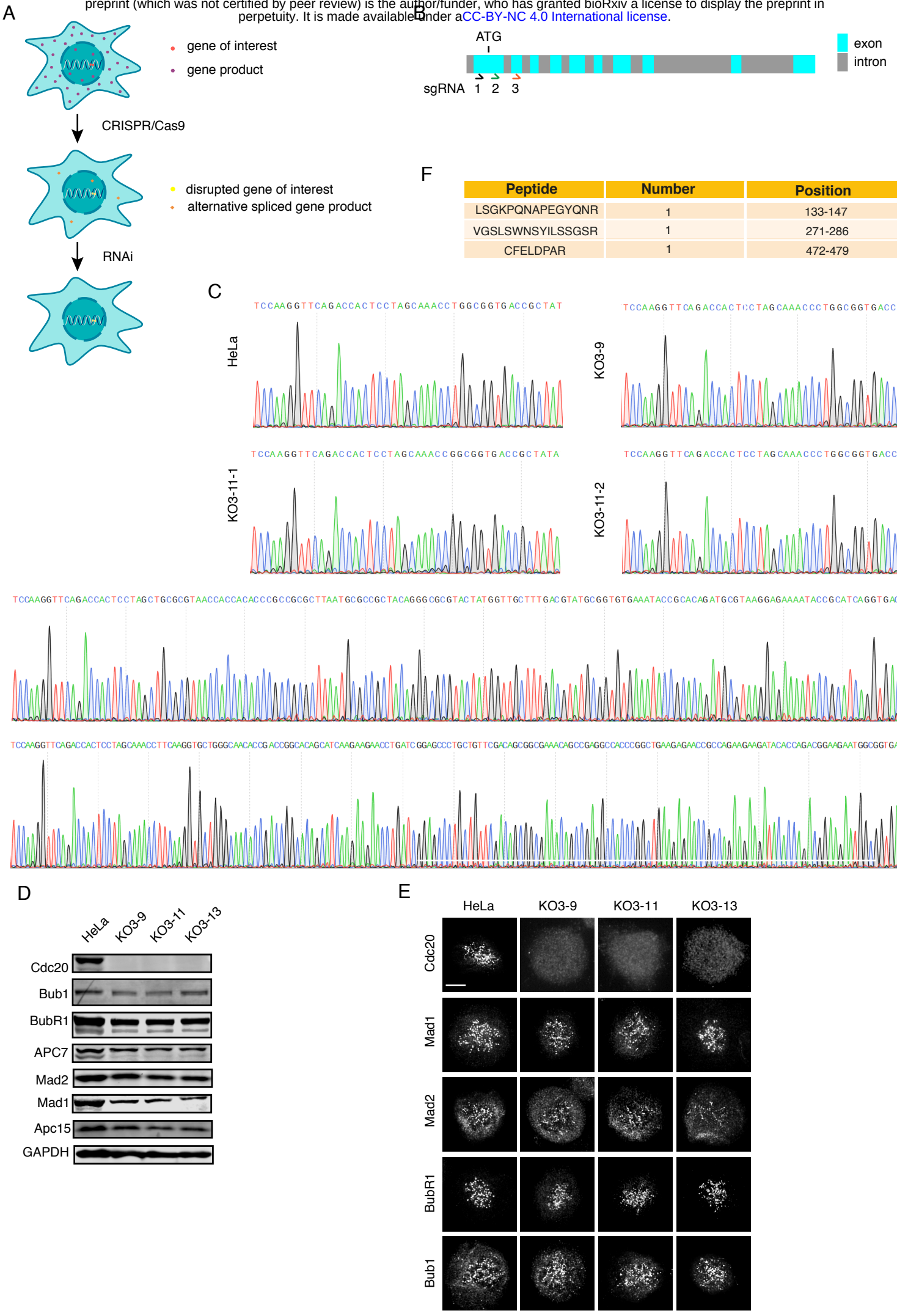

F

Peptide	Number	Position
LSGKPQNAPEGYQNR	1	133-147
VGSLSWNSYILSSGSR	1	271-286
CFELDPAR	1	472-479

Supplementary Figure 1

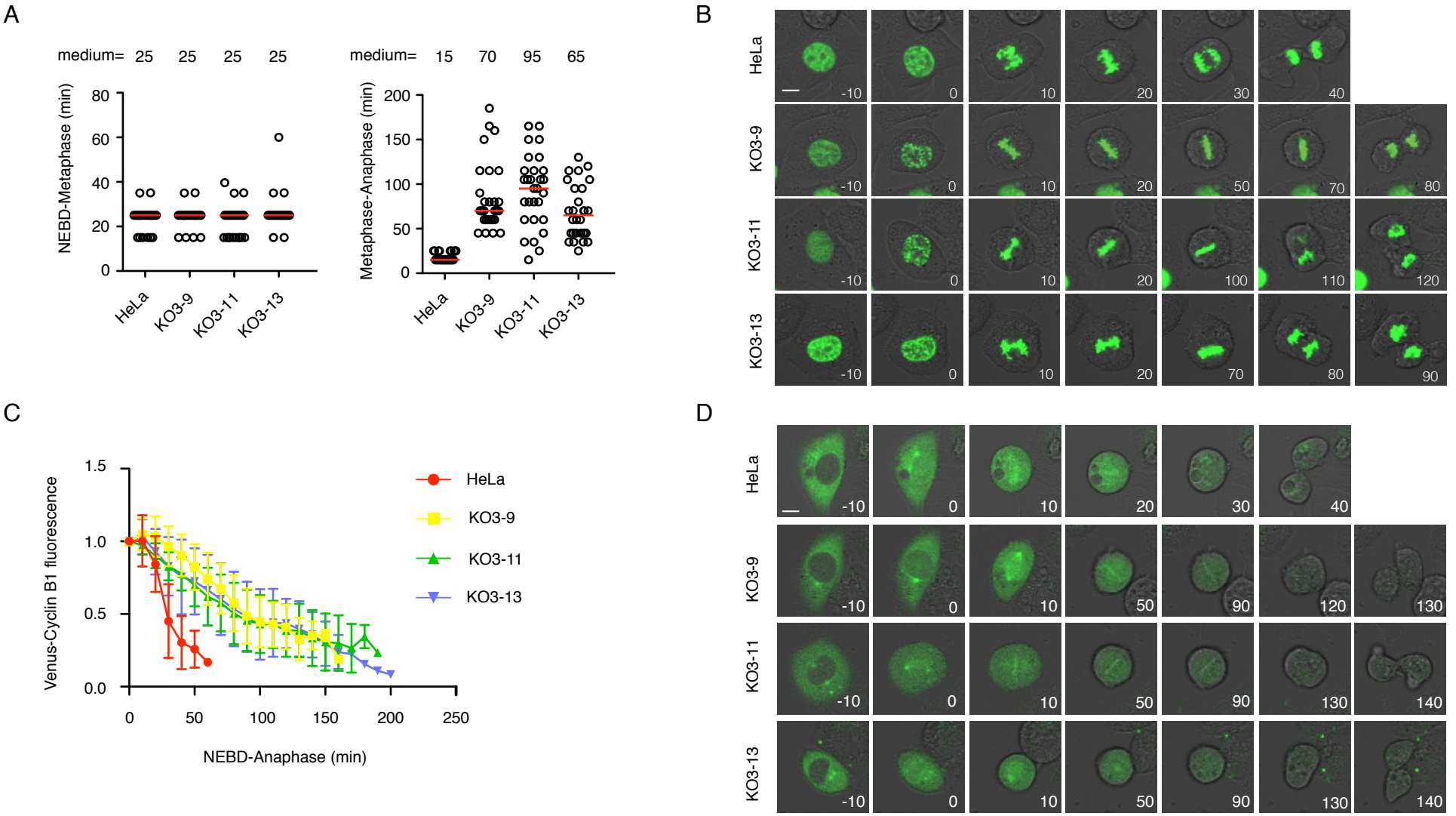

Supplementary Figure 2

A

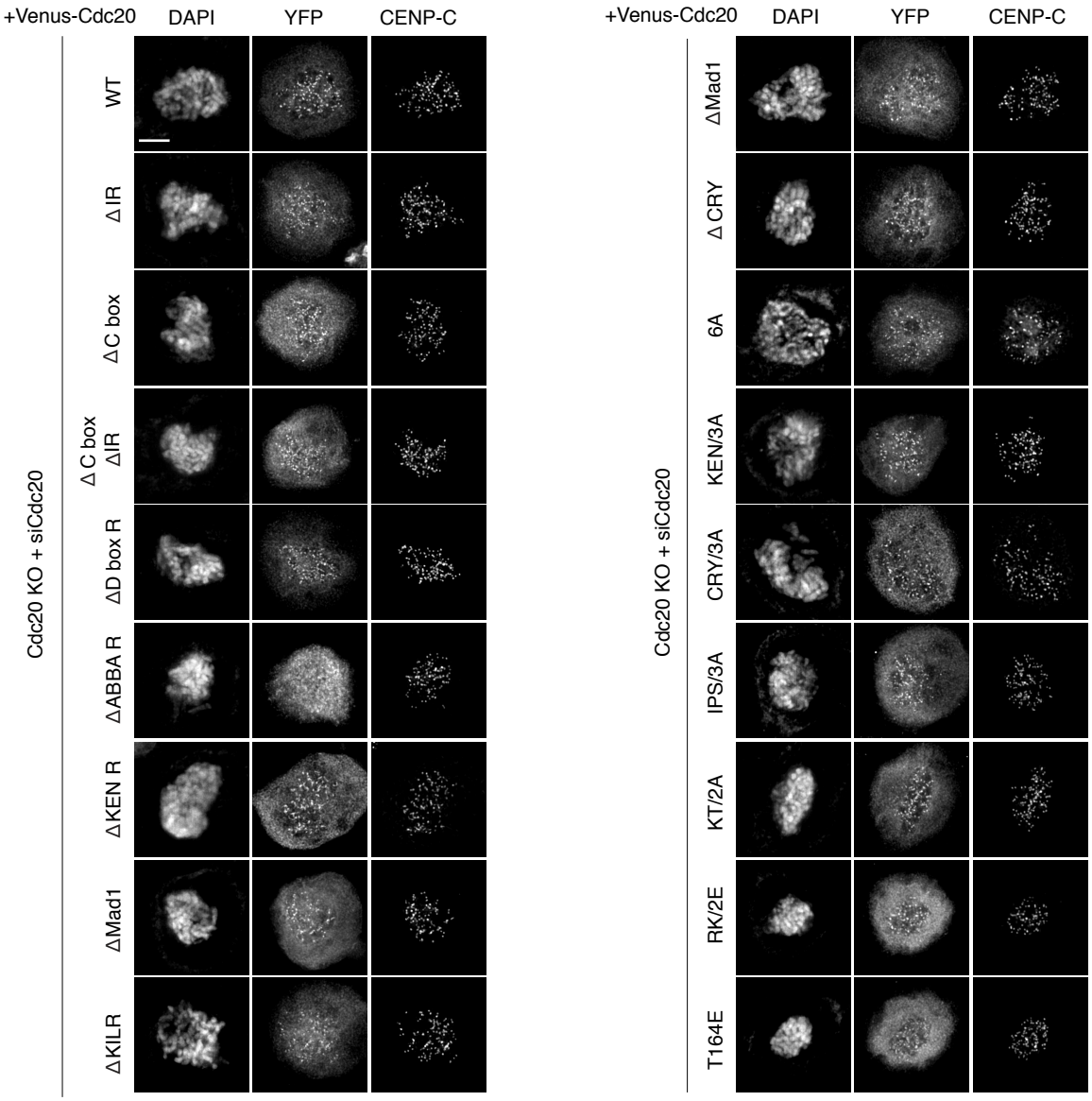

B

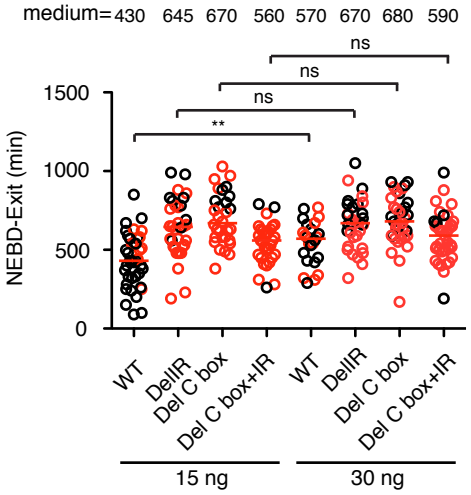

C

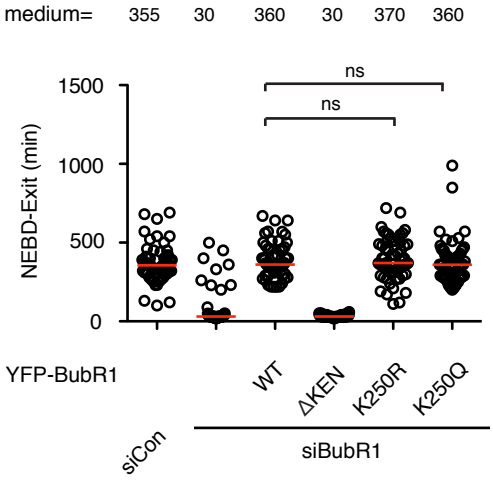

Supplementary Figure 3

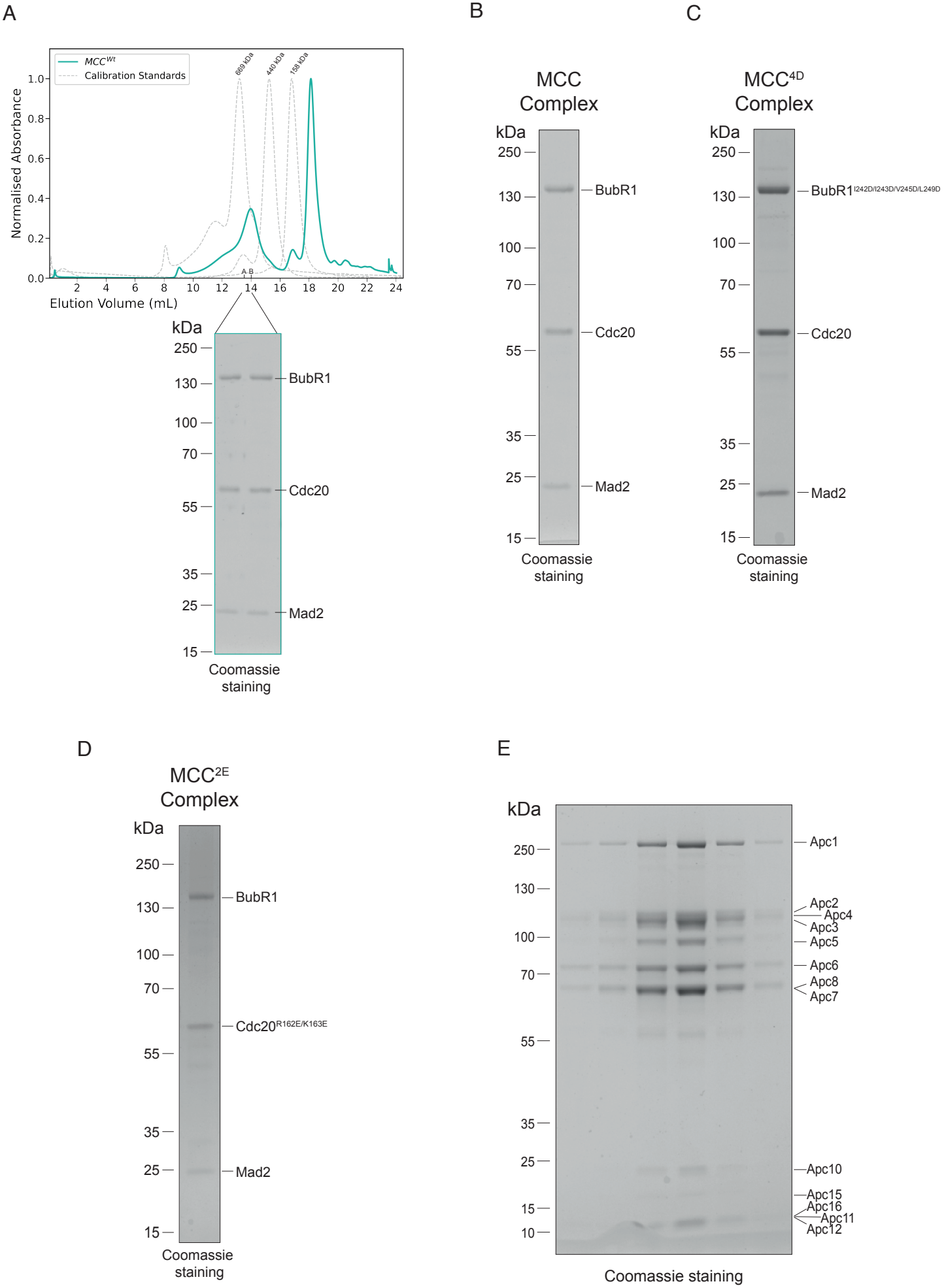

Supplementary Figure 4